Stoch Environ Res Risk Assess (2010) 24:725–733
DOI 10.1007/s00477-009-0359-2

ORIGINAL PAPER

A stochastic differential equation model for assessing drought and flood risks

Koichi Unami · Felix Kofi Abagale · Macarius Yangyuoru · Abul Hasan M. Badiul Alam · Gordana Kranjac-Berisavljevic

Published online: 26 November 2009

Abstract Droughts and floods are two opposite but related hydrological events. They both lie at the extremes of rainfall intensity when the period of that intensity is measured over long intervals. This paper presents a new concept based on stochastic calculus to assess the risk of both droughts and floods. An extended definition of rainfall intensity is applied to point rainfall to simultaneously deal with high intensity storms and dry spells. The mean-reverting Ornstein–Uhlenbeck process, which is a stochastic differential equation model, simulates the behavior of point rainfall evolving not over time, but instead with cumulative rainfall depth. Coefficients of the polynomial functions that approximate the model parameters are identified from observed raingauge data using the least squares method. The probability that neither drought nor flood occurs until the cumulative rainfall depth reaches a given value requires solving a Dirichlet problem for the backward Kolmogorov equation associated with the stochastic differential equation. A numerical model is developed to compute that probability, using the finite element method with an effective upwind discretization scheme. Applicability of the model is demonstrated at three raingauge sites located in Ghana, where rainfed subsistence farming is the dominant practice in a variety of tropical climates.

Keywords Point rainfall · Dry spell · Mean-reverting Ornstein–Uhlenbeck process · Backward Kolmogorov equation · Ghana

K. Unami (✉) · A. H. M. Badiul Alam
Graduate School of Agriculture, Kyoto University, Sakyo-ku, Kyoto 606-8502, Japan
e-mail: unami@adm.kais.kyoto-u.ac.jp

A. H. M. Badiul Alam
e-mail: alam@kais.kyoto-u.ac.jp

F. K. Abagale · G. Kranjac-Berisavljevic
Faculty of Agriculture, University for Development Studies, P. O. Box TL 1882, Tamale, Ghana
e-mail: fabagale@yahoo.com

G. Kranjac-Berisavljevic
e-mail: gordanak@gmail.com

M. Yangyuoru
Institute of Agricultural Research, University of Ghana, P. O. Box 68, Accra, Ghana
e-mail: macarius_y@yahoo.com

1 Introduction

Droughts and floods are two opposite natural hazards, but both fundamentally stem from precipitation irregularity. In contrast to physical hydrology, stochastic hydrology applies probability theory to represent the variability of precipitation for engineering purposes. Rainfall at a particular site, i.e., point rainfall, is the most basic stochastic hydrological quantity used to characterize floods and droughts. Standard methodologies are well established to deal with point rainfall data in terms of the relationship between duration and intensity in rainfall events, the return period of high intensity storms or dry spells, and time series patterns of storms (Elliot 1995). However, these conventional approaches do not consider point rainfall as a continuous stochastic process. Since the 1990s, the Bartlett–Lewis rectangular pulse model has become the prevalent method to describe the statistical structure of continuous point rainfall over the entire time domain on a wide range of scales (Onof et al. 2000; Koutsoyiannis and Mamassis 2001), but it still considers the arrival of a storm and variation in rainfall intensity during the storm as separate phenomena.

Bodo et al. (1987) reviewed stochastic differential equations (SDEs) applicable to hydrology in perspective and summarized fundamentals such as Markov processes, Itô's calculus, and forward and backward Kolmogorov equations that can be applied in hydrology. Since then, several authors have developed stochastic process models for point rainfall with considerably different methodologies. This is partly due to a vast variety of climates across the globe. Najem (1988) applied Markovian models to alternating wet and dry periods in Lebanon. Gyasi-Agyei and Willgoose (1999) examined a generalized hybrid model consisting of a binary chain and an autoregressive model in Australia. Gyasi-Agyei (1999) identified regional parameters for this model, using second harmonic Fourier series to represent the seasonal variation of some of the parameters. The ideas of the hybrid model were further explored for applications to diurnal cycles in point rainfall (Gyasi-Agyei 2001) and to disaggregation of daily rainfall into fine time scales (Gyasi-Agyei 2005; Gyasi-Agyei and Parvez Bin Mahbub 2007). Wu et al. (2006) applied continuous and stochastic methods to temporal patterns of rainfall events in Hong Kong. Mishra et al. (2009) characterized droughts in India's West Bengal. In a West African context, Cowden et al. (2008) successfully applied parsimonious stochastic process models to domestic rainwater harvesting. These diverse models, implicitly or explicitly, assume that sequential occurrence of wet and dry periods and temporal variation in rainfall intensity during each storm event are two independent stochastic processes. We unify the two here as a single mean-reverting Ornstein–Uhlenbeck (MROU) process. The MROU process was originally applied in financial engineering for modeling the temporal behavior of real interest rates (Evans et al. 1994) and of asset prices (Chiang et al. 1995). Electrical load behavior is strongly time-dependent, and Huang et al. (2003) modeled it as an MROU process with an equilibrium assumed to be a smooth function of time.

Practical applicability of SDEs is emphasized in conjunction with boundary value problems for their associated Kolmogorov equations. The backward Kolmogorov equation with appropriate Dirichlet boundary conditions governs first exit time distributions, which are key quantities in many areas of risk management and option pricing (Patie and Winter 2008). Spencer and Bergman (1993) compared numerical results for first passage exit time problems solving forward (Fokker–Planck) and backward Kolmogorov equations. In the field of climatology, Chu (2007) used the first exit time concept to detect the temporal variability of climate indices. However, no method is yet established to apply that concept for a deeper understanding of point rainfall.

Using an SDE as the principal model, this paper presents a new concept that leads to better understanding of the stochastic nature of point rainfall, in order to simultaneously assess the risk of droughts and floods. The concept is based on an extended definition of rainfall intensity at the full range of scale. The MROU process models behavior of rainfall intensity, taking not time but the cumulative rainfall depth as the principal independent variable. Then the risk of floods and droughts is assessed in terms of the probability that the rainfall intensity exits from a prescribed safety domain. The probability distributed over the domain is given as the solution to a Dirichlet problem of a backward Kolmogorov equation. A numerical model is developed to compute the probability, using the finite element method. The model is applied to data obtained from three raingauge sites under different agro-ecological climate zones of Ghana, where the dominant industry is rainfed subsistence farming and irregularity of rainfall is a prime concern. There are several studies in the literature dealing with West African point rainfall. Amani and Lebel (1998) statistically considered the reference mean areal rainfall that can be estimated from sparse raingauge networks. Lebel et al. (2000) demonstrated spatio-temporal variability of rainfall with different scales. However, this study focuses on time series data observed at individual raingauge sites. Computational methods are proposed to identify model parameters and to solve the Dirichlet problem, whose boundary condition in the time direction displays annual periodicity.

2 Stochastic process model

The cumulative rainfall depth at a fixed observation site is assumed to be a well-defined function of time t, and will be denoted by the notation $S = S(t)$ throughout this paper. Rainfall intensity $r = r(t)$ is understood to be the first derivative of S with respect to t. This relation is written in differential form

$$dS = r dt. \tag{1}$$

For a specified rainfall increment δ, the temporal duration T_δ satisfying

$$S(t) - S(t - T_\delta) = \delta \tag{2}$$

is another function of t and is referred to as the incremental rainfall duration. From this T_δ, the temporal variable X is defined as

$$X = \log \frac{\delta}{T_\delta} \tag{3}$$

and is considered stochastic. The relation between S and r in Eq. 1 is inverted and approximated as

$$\mathrm{d}t = \frac{1}{r}\mathrm{d}S \approx \frac{T_\delta}{\delta}\mathrm{d}S = \exp(-X)\mathrm{d}S \tag{4}$$

since $\frac{\delta}{T_\delta}$ approaches r as δ approaches 0. The stochastic variable X becomes smaller or larger during a drought or a flood but reverts to an average when such an event ends. The MROU process is the simplest model having this property of mean reversion and is the solution of the SDE

$$\mathrm{d}X = K(\beta - X)\mathrm{d}S + \sqrt{v}\mathrm{d}B_S \tag{5}$$

where K is the decay coefficient, β the mean reversion level, $\sqrt{v}$ the volatility, and B_S is the canonical Brownian motion evolving with S.

3 Identification of model parameters

An explicit function $\bar{F}$, which is a P-periodic trigonometric polynomial of t and a polynomial of X, approximates a generic model parameter F as

$$\bar{F}(t,X) = \sum_{i=0}^{n_X}\left[\left\{f_{i,0} + \sum_{k=1}^{n_t}\left(f_{i,2k-1}\cos\frac{2\pi kt}{P} + f_{i,2k}\cos\frac{2\pi kt}{P}\right)\right\}X^i\right] \tag{6}$$

where n_X is the degree of the polynomial, i the index for terms of polynomial, n_t the degree of trigonometric polynomial, k the index for terms of trigonometric polynomial, and the $f_{i,*}$ terms are coefficients for a generic integer index *. Normally, one year is the dominant period P for long-term precipitation series. The coefficients $f_{i,*}$ are determined by the least squares method

$$J_F = \frac{1}{2}\sum_{j=1}^{n}\left(\bar{F}(t_j,X_j) - \hat{F}(t_j,X_j)\right)^2 \tag{7}$$

where J_F is the sum of squared residuals to be minimized, j the index of data, n the number of available data, and $\hat{F}$ is the value of F estimated from the data.

The decay coefficient K, the mean reversion level β, and the volatility $\sqrt{v}$ are model parameters to be identified. Practically, however, logarithmic transformations are applied and we seek to identify $\kappa = \log K$ and $\psi = \log v$ instead of pursuing the skewed model parameters K and $\sqrt{v}$ directly.

Firstly, assuming that X is reverting to its own average value, approximation of β is implemented with

$$\hat{\beta} = X. \tag{8}$$

Then, the other model parameters are approximated in the context of a discrete version of Eq. 5, which is written as

$$X^+ - X = K(\beta - X)(S^+ - S) + \sqrt{v}\Delta B_S \tag{9}$$

where the superscript + denotes the value after an incremental time Δt, and ΔB_S is the corresponding increment of B_S. Applying the triangle inequality and Itô's rule to Eq. 9 results in

$$\frac{|X^+ - X| - \sqrt{v|S^+ - S|}}{|\beta - X|(S^+ - S)} \le K \le \frac{|X^+ - X| + \sqrt{v|S^+ - S|}}{|\beta - X|(S^+ - S)} \tag{10}$$

then $\hat{\kappa}$ is set as

$$\hat{\kappa} = \log\frac{|X^+ - X|}{|\beta - X|(S^+ - S)}. \tag{11}$$

On the other hand, squaring both sides of Eq. 9 with Itô's rule yields

$$\hat{\psi} = \log\frac{(X^+ - X)^2}{S^+ - S}. \tag{12}$$

4 The Dirichlet problem

The Dirichlet problem is formulated after Øksendal (2005).

The SDE (Eq. 5) and the ordinary differential equation (Eq. 4) with the trivial relation $\mathrm{d}S = \mathrm{d}S$ are summarized in vector form as

$$\begin{pmatrix}\mathrm{d}S\\ \mathrm{d}t\\ \mathrm{d}X\end{pmatrix} = \begin{pmatrix}1\\ \exp(-X)\\ K(\beta - X)\end{pmatrix}\mathrm{d}S + \begin{pmatrix}0\\ 0\\ \sqrt{v}\end{pmatrix}\mathrm{d}B_S. \tag{13}$$

The generator A is deduced as

$$A = \frac{\partial}{\partial s} + \exp(-x)\frac{\partial}{\partial t} + K(\beta - x)\frac{\partial}{\partial x} + \frac{v}{2}\frac{\partial^2}{\partial x^2} \tag{14}$$

where s and x are the real numbers representing the values of S and X, respectively. The domain D of s, t, and x is taken as $(-\infty, 0) \times (-\infty, \infty) \times \Omega$, prescribing the domain Ω in the x-direction as $(X_{\mathrm{inf}}, X_{\mathrm{sup}})$ where X_{inf} is the drought level and X_{sup} is the flood level. The function $u = u(s, t, x)$ satisfying the backward Kolmogorov equation

$$Au = \frac{\partial u}{\partial s} + \exp(-x)\frac{\partial u}{\partial t} + K(\beta - x)\frac{\partial u}{\partial x} + \frac{v}{2}\frac{\partial^2 u}{\partial x^2} = 0 \tag{15}$$

in D with the Dirichlet conditions

$$u(0,t,x) = 1, \tag{16}$$

$$u(s,t,X_{\mathrm{inf}}) = u\left(s,t,X_{\mathrm{sup}}\right) = 0, \tag{17}$$

and

$$u(s,t,x) = u(s,t+P,x) \tag{18}$$

is interpreted as the probability that the stochastic variable X remains in its domain Ω until the cumulative rainfall depth in the interval following the current time t reaches $-s = |s|$.

5 Numerical model

The finite element method is commonly used in numerical modeling to address approximate solutions for partial differential equations with boundary conditions. A finite number of test functions are substituted for the weight in the weak form of the partial differential equation. The choice of test functions is referred to as the discretization scheme and determines the performance of the numerical model.

The partial differential equation Eq. 15 with the boundary conditions prescribed in Eq. 17 is rewritten in the weak form

$$\int_\Omega \left(w\frac{\partial u}{\partial s} + w\exp(-x)\frac{\partial u}{\partial t} + wK(\beta - x)\frac{\partial u}{\partial x} - \frac{1}{2}\frac{\partial (wv)}{\partial x}\frac{\partial u}{\partial x} \right) \mathrm{d}x = 0 \tag{19}$$

for any weight $w \in H_0^1(\Omega)$, which is the space of functions having certain regularity properties in Ω and vanishing at the boundary of Ω. An effective upwind discretization scheme is proposed here, dividing the domain Ω into n subdomains of equal length $\Delta x = \frac{X_{\sup} - X_{\inf}}{n}$. The kth node falls on $X_{\inf} + k\Delta x$ and is denoted by x_k. The weight w for the generic kth node in the scheme is set as

$$w = \frac{1}{v}\varphi_k \tag{20}$$

where φ_k is an upwind function defined as

$$\varphi_k = \begin{cases} \left(\frac{x - x_{k-1}}{\Delta x}\right)^{p_k^l} & (x_{k-1} < x \le x_k) \\ \left(\frac{x_{k+1} - x}{\Delta x}\right)^{p_k^r} & (x_k < x \le x_{k+1}) \\ 0 & (\text{Otherwise}) \end{cases} \tag{21}$$

with

$$p_k^l = \exp(Pe^l) \tag{22}$$

and

$$p_k^r = \exp(-Pe^r) \tag{23}$$

where the local Peclet numbers Pe^l and Pe^r are evaluated at $x_{k-\frac{1}{2}} = \frac{x_{k-1} + x_k}{2}$ and at $x_{k+\frac{1}{2}} = \frac{x_k + x_{k+1}}{2}$ as

$$Pe^l = \frac{K(t)\left(\beta(t) - x_{k-\frac{1}{2}}\right)\Delta x}{v\left(t, x_{k-\frac{1}{2}}\right)} \tag{24}$$

and

$$Pe^r = \frac{K(t)\left(\beta(t) - x_{k+\frac{1}{2}}\right)\Delta x}{v\left(t, x_{k+\frac{1}{2}}\right)}, \tag{25}$$

respectively. Examples of the upwind functions are depicted in Fig. 1. This setting of weights results in

$$\int_\Omega \left(\frac{\Delta x}{v}\varphi_k \frac{\partial u}{\partial s} + \frac{\exp(-x)\Delta x}{v}\varphi_k \frac{\partial u}{\partial t} + Pe\varphi_k \frac{\partial u}{\partial x} - \frac{\Delta x}{2}\frac{\partial \varphi_k}{\partial x}\frac{\partial u}{\partial x} \right) \mathrm{d}x = 0. \tag{26}$$

Taking the signs of the coefficients into account, the partial derivatives $\frac{\partial u}{\partial s}$ and $\frac{\partial u}{\partial t}$ are implicitly approximated as

$$\frac{\partial u}{\partial s} \approx \frac{u_{i-1,j}(x) - u_{i,j}(x)}{\Delta s} \tag{27}$$

$$\frac{\partial u}{\partial t} \approx \frac{u_{i,j+1}(x) - u_{i,j}(x)}{\Delta t} \tag{28}$$

where Δs is the increment in the s-direction, Δt is the increment in the t-direction and is equal to $\frac{P}{m}$ for a prescribed temporal step number m, and u is linearly interpolated in the x-direction as

$$u_{i,j}(x) = u_{i,j,k} + \left(u_{i,j,k+1} - u_{i,j,k}\right)\frac{x - x_k}{\Delta x} \tag{29}$$

with

$$u_{i,j,k} = u(-i\Delta s, j\Delta t, x_k). \tag{30}$$

The linear interpolation Eq. 29 in the x-direction discretizes the integrals in Eq. 26 as

$$\int_\Omega f\varphi_k u_{i,j}(x)\mathrm{d}x = \Delta x \left\langle \begin{pmatrix} \frac{f_{k-1}}{(p_k^l+1)(p_k^l+2)} \\ \frac{f_k}{p_k^l+2} + \frac{f_k}{p_k^r+2} \\ \frac{f_{k+1}}{(p_k^r+1)(p_k^r+2)} \end{pmatrix}, \begin{pmatrix} u_{i,j,k-1} \\ u_{i,j,k} \\ u_{i,j,k+1} \end{pmatrix} \right\rangle \tag{31}$$

where f is $\frac{1}{v}$ or $\frac{\exp(-x)}{v}$ and the superscript represents the node number where f is evaluated,

$$\int_\Omega Pe\varphi_k \frac{\partial}{\partial x}u_{i,j}(x)\mathrm{d}x = \left\langle \begin{pmatrix} -\frac{Pe^l}{p_k^l+1} \\ \frac{Pe^l}{p_k^l+1} - \frac{Pe^r}{p_k^r+1} \\ \frac{Pe^r}{p_k^r+1} \end{pmatrix}, \begin{pmatrix} u_{i,j,k-1} \\ u_{i,j,k} \\ u_{i,j,k+1} \end{pmatrix} \right\rangle, \tag{32}$$

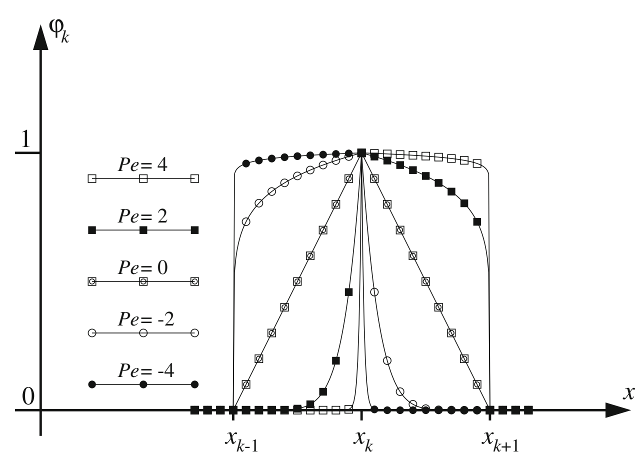

Fig. 1 Upwind functions for different local Peclet numbers

and

$$\int_{\Omega} \frac{\partial \varphi_k}{\partial x} \frac{\partial u_{i,j}(x)}{\partial x} \mathrm{d}x = \frac{1}{\Delta x} \left\langle \begin{pmatrix} -1 \\ 2 \\ -1 \end{pmatrix}, \begin{pmatrix} u_{i,j,k-1} \\ u_{i,j,k} \\ u_{i,j,k+1} \end{pmatrix} \right\rangle \qquad (33)$$

where $\langle \mathbf{v}, \mathbf{w} \rangle$ denotes the inner product between generic three-dimensional vectors $\mathbf{v}$ and $\mathbf{w}$. Finally, Eq. 26 is transformed into a linear equations system

$$M\mathbf{u} = G_s \mathbf{u}^{s+} + G_t \mathbf{u}^{t+} \qquad (34)$$

where $\mathbf{u}$, $\mathbf{u}^{s+}$, and $\mathbf{u}^{t+}$ are the $n-1$-dimensional vectors whose kth entries are $u_{i,j,k}$, $u_{i-1,j,k}$, and $u_{i,j+1,k}$, respectively. Corresponding to the conditions of Eqs. 16 and 18, Eq. 34 is solved with

$$u_{0,j,k} = 0 \qquad (35)$$

and

$$u_{i,m,k} = u_{i,0,k}. \qquad (36)$$

6 Applications

Using the data obtained from the Ghanaian raingauge sites, the model's applicability is demonstrated. Since the purpose here is to present a new concept, only the cases where the minimum and the maximum observed values of X are set as X_{inf} and X_{sup}, respectively, are considered.

6.1 Rain gauge sites

Figure 2 delineates the agro-ecological zones and river drainage system of Ghana, which is a West African country along the Gulf of Guinea. In general the climate is drier in the northern parts of the country, but the south-eastern coastal savanna receives the scantiest mean annual rainfall. The dominant rainfall types in Ghana are squall line precipitation in the south and local convective rain in the north (Jenkins et al. 2002). Owusu and Waylen (2009) have reported statistics of annual rainfall totals at several Ghanaian stations. A comparison of two periods: 1951–1970 and 1981–2000 for the Tamale and Accra stations is shown in Table 1. Downward trends in annual rainfall totals were confirmed at most of the stations.

The three raingauge sites considered in this paper are referred to as Gung, Kade, and Legon, and their locations are also shown in Fig. 2. The Gung and Legon sites are in the suburbs of the Tamale and Accra metropolitan areas, respectively. The raingauge installed at each site is of the same tipping-bucket type and is connected to a pulse logger, which records a series of $t = t_0,\ t_1,\ \ldots$ such that $t_{k+1} - t_k = T_\delta$ with $\delta = 0.2$ mm. However, the observation periods are different for the sites for technical reasons. The next section contains a description of each site.

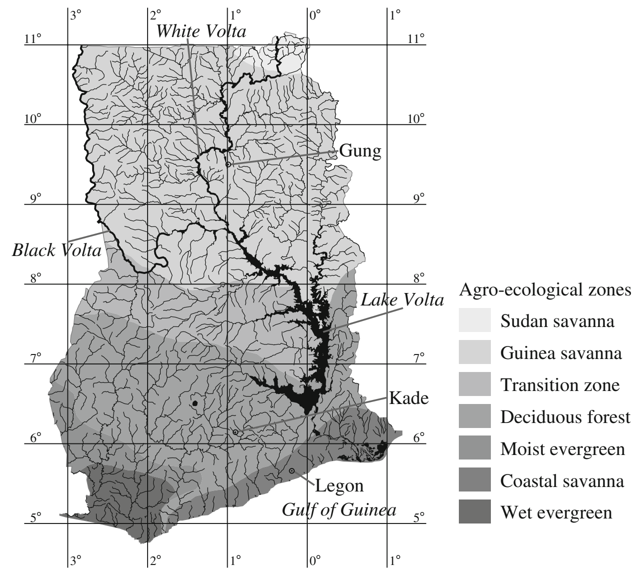

Fig. 2 Agro-ecological zones and river drainage system of Ghana with locations of raingauges

Table 1 Mean and standard deviation (SD) of annual rainfall totals in different periods

Station	1951–1970		1981–2000	
	Mean (mm)	SD (mm)	Mean (mm)	SD (mm)
Tamale	1,144	266	1,061	215
Accra	926	233	669	192

6.1.1 Gung

Gung is a rural community in the Tolon/Kumbungu District of the Northern Region of Ghana. It is situated in the basin of the Bontanga River, a tributary of the White Volta River. The area is in the Guinea savanna agro-ecological zone, where annual rainfall pattern is monomodal with a single rainy season from mid-March to October. The site is located at coordinates 09°29′57″N 000°59′17″W, about 700 m distant from the Gung community. Rain gauge data from September 1, 2005 to October 27, 2008 were used. Figure 3 shows the monthly rainfall depths within this period. There was almost no rain during the dry season from November to mid-March. The total annual rainfall depths were 666.4 mm in 2006, 861.4 mm in 2007, and 1008.0 mm in 2008. Based on statistics for the period from 1981 to 2000 shown in Table 1, the rainfall in 2008 was within normal limits while that in 2006 was very low for the area. In 2007, dry spells were prolonged in the early stages of the growing season, but severe floods followed in September. Unami et al. (2009) hydraulically analyzed the runoff processes during the 2007 September floods in a

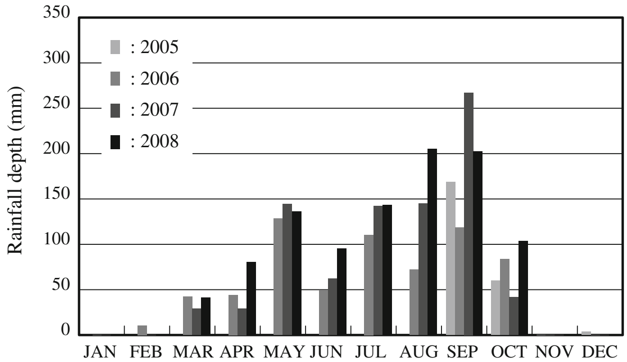

Fig. 3 Monthly rainfall depths observed at the Gung site

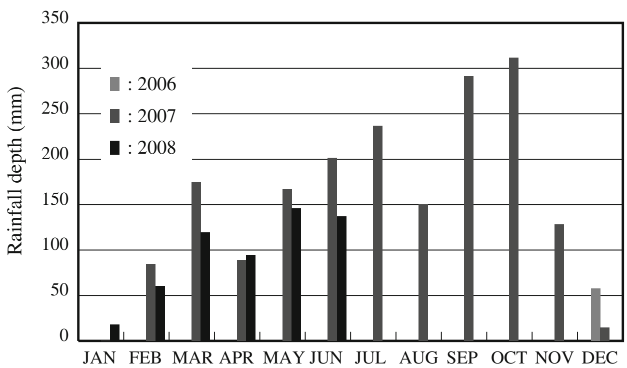

Fig. 4 Monthly rainfall depths observed at the Kade site

nearby inland valley. The domain Ω of x is set as $\left(X_{\inf}, X_{\sup}\right) = (-9.70, 5.48) = \left(\log \frac{\delta}{137\text{days}}, 240\ \text{mm/h}\right)$.

6.1.2 Kade

A raingauge was installed at the Agricultural Research Centre (ARC)-Kade, University of Ghana. The site coordinates are 06°08′32″N 000°53′57″W, falling on the northwest side of Kade township, in the Eastern Region of Ghana. ARC-Kade specializes in experimental research on tree crops being cultivated in the deciduous forest agro-ecological zone, where rainfall is more abundant than in the savanna zones. According to Lawson et al. (1970), the annual rainfall pattern peaks in July and October with a yearly total of 1,686 mm. Rain gauge data from November 10, 2006 to August 23, 2008 were used, so the only calendar year with complete data was 2007. Figure 4 shows the monthly rainfall depths during the period. The total rainfall depth in 2007 was 1,849.4 mm, though no rain was observed in January. The domain Ω of x is set as $\left(X_{\inf}, X_{\sup}\right) = (-8.32, 5.66) = \left(\log \frac{\delta}{34.4\text{days}}, 288\text{mm/hour}\right)$.

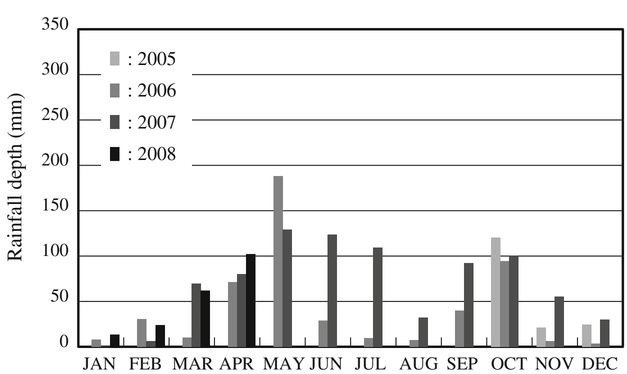

Fig. 5 Monthly rainfall depths observed at the Legon site

6.1.3 Legon

The main campus of the University of Ghana is at Legon, in the northeastern area of Accra, the capital of Ghana. Accra lies in the coastal savanna agro-ecological zone having a bimodal rainfall pattern, with major and minor rainy seasons from March to July and from September to November,

Table 2 Dimensions and estimates of model parameters

F	n_X	n_t	$\hat{F}$	Δt
$\kappa = \log K$	0	2	$\frac{\lvert X^{+} - X\rvert}{\lvert \beta - X\rvert (S^{+} - S)}$	T_{δ}
β	0	3	X	10 s
$\psi = \log v$	2	2	$\log \frac{(X^{+} - X)^2}{S^{+} - S}$	10 s

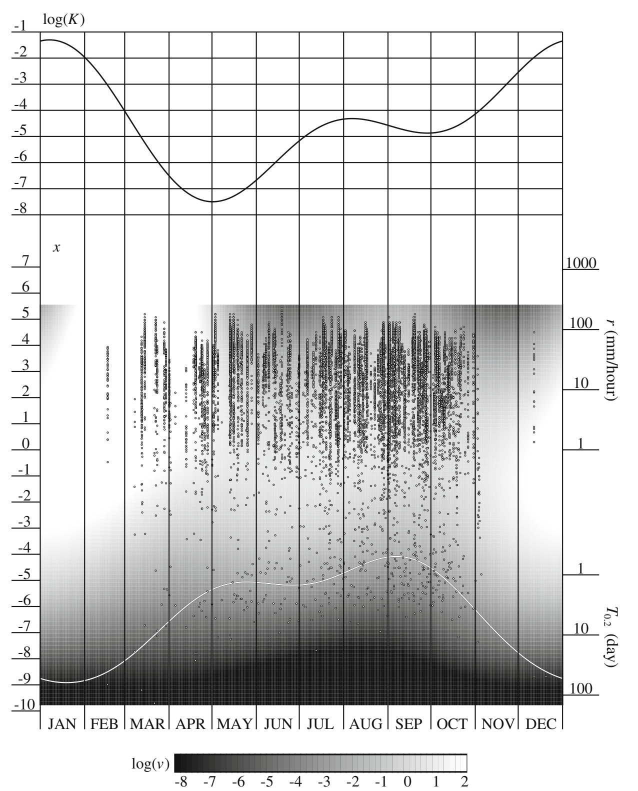

Fig. 6 Observed X (*bullets*) and identified model parameters for the Gung site. The *black curve* represents $\kappa = \log(K)$, the *white curve* β, and the *gray shading* $\psi = \log(v)$

respectively. The raingauge was set in the students' experimental plot area of the School of Agriculture, at coordinates 05°39′35″N 000°11′37″W. Rain gauge data from September 6, 2005 to May 15, 2008 were used, giving two full calendar years of data, for 2006 and 2007. Figure 5 shows the monthly rainfall depths within the period. The annual rainfall depth in 2006 was low at 499.4 mm, but normal in 2007 at 828.2 mm. The domain Ω of x is set as $(X_{\inf}, X_{\sup}) = (-8.29, 6.17) = \left(\log \frac{\delta}{33.2\ \text{days}}, 480\ \text{mm/h}\right)$.

6.2 Results of parameter identification

The model parameters $\kappa = \log(K)$, β, and $\psi = \log v$ for each of the sites were identified from the observed data. The period P is fixed as 365.25 days, because auto-correlation functions based on daily and monthly data support the notion that significant variations in rainfall for all the sites are best understood as yearly patterns. The minimum degrees of the polynomials are chosen as shown in Table 2, so that spurious oscillation does not occur in the variation of the model parameters. The incremental time Δt for identification is taken as T_δ for κ, but it is fixed as 10 s for β and ψ since most of the data are lie in storm event periods. The results are displayed in Figs. 6, 7, and 8 for Gung, Kade, and Legon sites, respectively. All the model parameters are functions of t for a one-year period, but ψ depends on x as well. Being the average of X, β itself lies in the x-domain.

The decay coefficient K is large during the dry season in Gung and at the end of the major rainy season in Legon. It is small throughout the year in Kade. The mean reversion level β does not strictly follow the annual rainfall pattern at any of the sites because it contains information about dry spells as well. Volatility $\sqrt{v}$ is very small when X is close to the minimum and is large when X is large during the rainy seasons.

6.3 Numerical solution of Dirichlet problem

Using the numerical model, $u_{i,j,k}$ for $0 < i \leq N = 50,000$ is computed with $\Delta s = 0.02$ mm, $m = 365$, and $n = 100$. The results at $i = N$, which corresponds to $s = -N\Delta s = -1{,}000$ mm, for the Gung, Kade, and Legon sites are shown in Figs. 9, 10, and 11, respectively. The mean reversion level β and the observed X are also plotted. This $u_{N,j,k}$ is the probability that the stochastic variable X, which is found to be x at the current time t, becomes neither the drought level $X_{\inf}$ nor the flood level $X_{\sup}$ until the cumulative rainfall

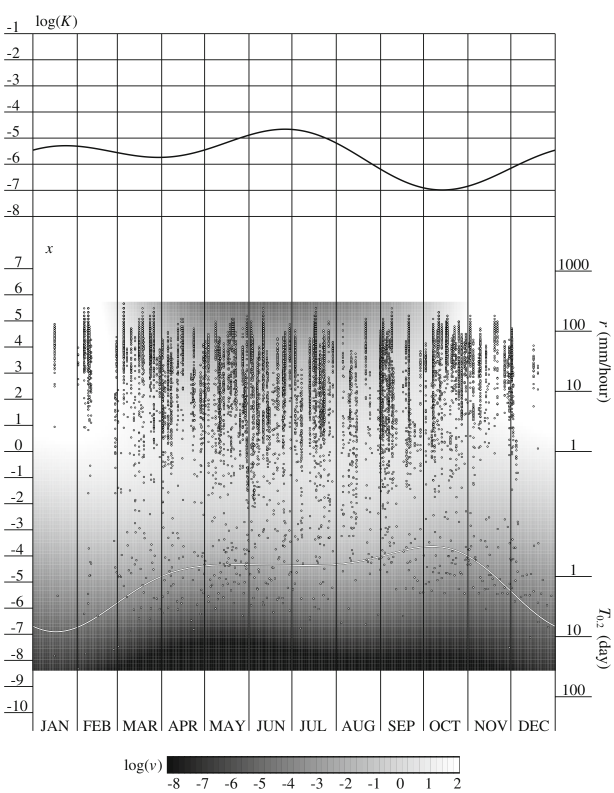

Fig. 7 Observed X (*bullets*) and identified model parameters for the Kade site. The *black curve* represents $\kappa = \log(K)$, the *white curve* β, and the *gray shading* $\psi = \log(v)$

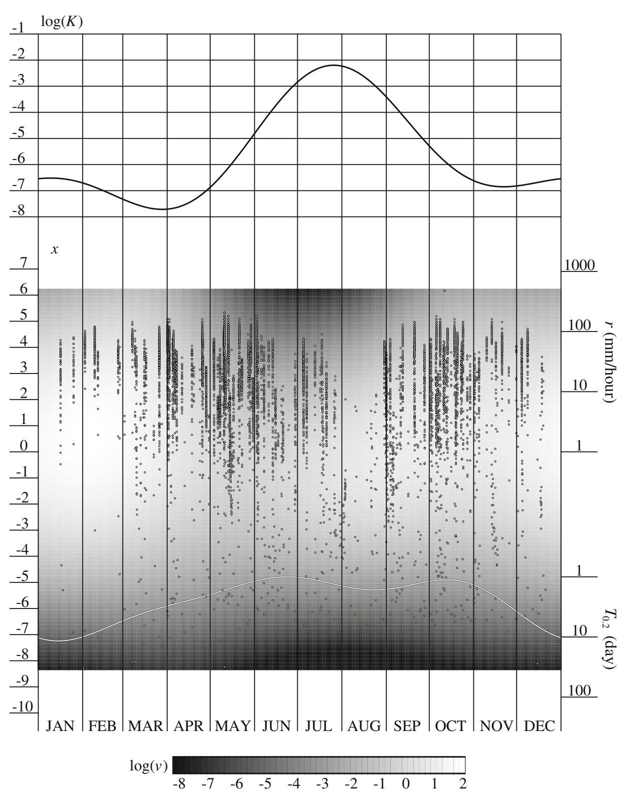

Fig. 8 Observed X (*bullets*) and identified model parameters for the Legon site The *black curve* represents $\kappa = \log(K)$, the *white curve* β, and the *gray shading* $\psi = \log(v)$

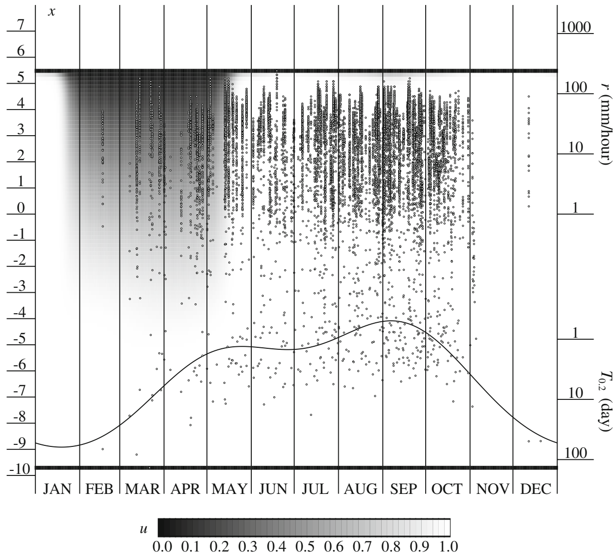

Fig. 9 Computational results for the Gung site

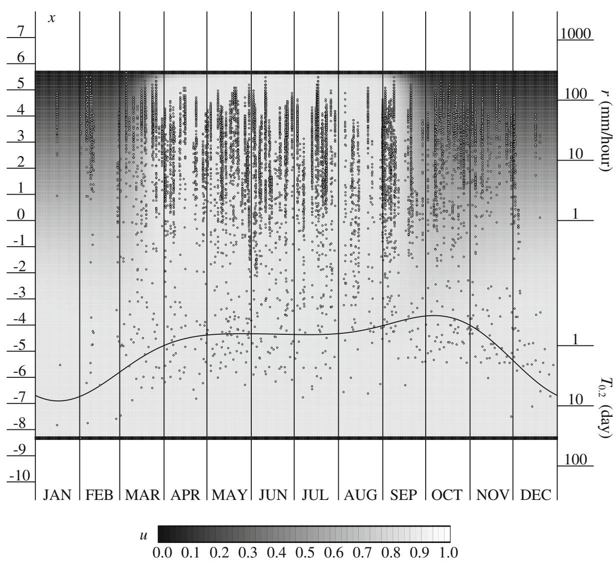

Fig. 10 Computational results for the Kade site

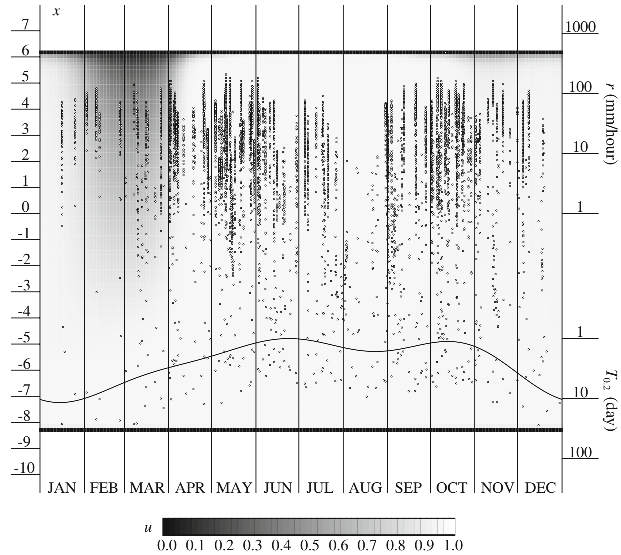

Fig. 11 Computational results for the Legon site

depth S in the interval following the current time t reaches 1,000 mm. Irrespective of the homogeneous boundary condition of Eq. 17, the probability is high and almost constant when x is close to or less than β, with values of 1.00, 0.86, and 0.95 for Gung, Kade, and Legon sites, respectively. Conversely dry spells can be interpreted as having occurred when the respective observation periods are long. The probability is very low that high rainfall intensity will actually be observed during the dry seasons, as X is likely to reach $X_{\sup}$ because the volatility $\sqrt{v}$ is large.

Two indices, J_∞ and J_2, representing the magnitude of $u_{i,j,k}$ for a given i are defined as

$$J_\infty = \max_{j,k} \left| u_{i,j,k} \right| \tag{37}$$

and

$$J_2 = \frac{1}{(n-1)m} \sum_{j=0}^{m-1} \sum_{k=1}^{n-1} \left| u_{i,j,k} \right|^2, \tag{38}$$

respectively. Their variation with i is shown in Fig. 12. For the Gung site, where the effect of mean reversion is strong and the volatility $\sqrt{v}$ is small in the relevant domain of t and x, the numerical solution $u_{N,j,k}$ is generally steady with respect to i. This is not the case for the other two sites, where $u_{i,j,k}$ gradually converges to the trivial steady solution $u_{\infty,j,k} = 0$.

7 Conclusions

The SDE model, together with the computational methods used here, provides a new stochastic approach to point rainfall data. It is utilized for assessing the risk of droughts and floods. The most innovative point is that the principal independent variable is not time but the cumulative rainfall depth. Drought and flood levels define a single computational domain, where the Dirichlet problem is solved in the x-direction. The concept is so fundamental that only one computational example is demonstrated for each raingauge site. Characteristics of the rainfall at each site can be seen from the distribution of the model parameters, although the identification method still needs to be improved.

The concept could have a variety of applications besides that demonstrated in this paper. Setting the domain Ω differently may result in totally different behavior of the

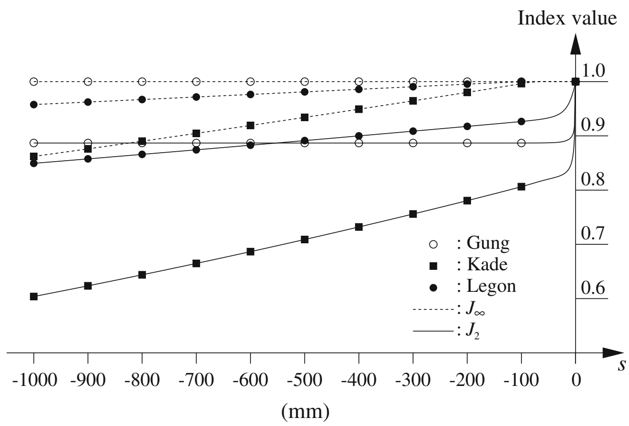

Fig. 12 Magnitude of probability changing with s for each site

probability. If $X_{\inf}$ is large enough or $X_{\sup}$ is small enough, the probability $u_{i,j,k}$ quickly converges to the trivial steady solution $u_{\infty,j,k} = 0$. The maximum rainfall intensity and the maximum length of dry spell are often needed in design problems, and they can be identified as the boundaries of the smallest domain Ω such that a non-trivial steady solution of the probability exists. When the growing period of a particular rainfed crop is set as the domain in the t-direction in place of imposing the periodic boundary condition, the probability would measure the chance of having a successful harvest not affected by a drought or flood. This will be an important application for assessing food security in subsistence farming areas where the length of the growing season is limited.

Acknowledgements This research was supported by a grant-in-aid for scientific research No.20255012, from the Japan Society for the Promotion of Science.

References

Amani A, Lebel T (1998) Relationship between point rainfall, average sampled rainfall and ground truth at the event scale in Sahel. Stoch Hydrol Hydraul 12:141–154

Bodo BA, Thompson ME, Unny TE (1987) A review on stochastic differential equations for applications in hydrology. Stoch Hydrol Hydraul 1:81–100

Chiang R, Liu P, Okunev J (1995) Modelling mean reversion of asset prices toward their fundamental value. J Banking Financ 19:1327–1340

Chu PC (2007) First passage time analysis on climate indices. J Atmos Ocean Technol 25:258–270

Cowden JR, Watkins DW Jr, Mihelcic JR (2008) Stochastic rainfall modeling in West Africa: parsimonious approaches for domestic rainwater harvesting assessment. J Hydrol 361:64–77

Elliot WJ (1995) Precipitation, chap 2 in Environmental hydrology, pp 19–50. CRC Press, Inc., FL

Evans LT, Keef SP, Okunev J (1994) Modelling real interest rates. J Banking Financ 18:153–165

Gyasi-Agyei Y (1999) Identification of regional parameters of a stochastic model for rainfall disaggregation. J Hydrol 223:148–163

Gyasi-Agyei Y (2001) Modelling diurnal cycles in point rainfall properties. Hydrol Process 15:595–608

Gyasi-Agyei Y (2005) Stochastic disaggregation of daily rainfall into one-hour time scale. J Hydrol 309:178–190

Gyasi-Agyei Y, Parvez Bin Mahbub SM (2007) A stochastic model for daily rainfall disaggregation into fine time scale. J Hydrol 347:358–370

Gyasi-Agyei Y, Willgoose GR (1999) Generalisation of a hybrid model for point rainfall. J Hydrol 223:148–163

Huang MX, Tao XH, Han ZX (2003) An electricity price model with consideration to load and gas price effects. J Zhejiang Univ Sci 4(6):666–671

Jenkins GS, Adamou G, Fongang S (2002) The challenges of modeling climate variability and change in West Africa. Clim Change 52(3):263–286

Koutsoyiannis D, Mamassis N (2001) On the representation of hyetograph characteristics by stochastic rainfall models. J Hydrol 251:65–87

Lawson GW, Armstrong-Mensah KO, Hall JB (1970) A catena in tropical moist semi-deciduous forest near Kade, Ghana. J Ecol 58(2):371–398

Lebel T, Delclaux F, Le Barbé L, Polcher J (2000) From GCM scales to hydrological scales: rainfall variability in West Africa. Stoch Environ Res Risk Assess 14:275–295

Mishra AK, Singh VP, Desai VR (2009) Drought characterization: a stochastic approach. Stoch Environ Res Risk Assess 23:41–55

Najem W (1988) A continuous point process model for daily rainfall. Stoch Hydrol Hydraul 2:189–200

Øksendal B (2005) Stochastic differential equations, 6th edn, pp 179–190. Springer, Berlin

Onof C, Chandler RE, Kakou A, Northrop P, Wheater HS, Isham V (2000) Rainfall modeling using Poisson-cluster processes: a review of developments. Stoch Environ Res Risk Assess 14:384–441

Owusu K, Waylen P (2009) Trends in spatio-temporal variability in annual rainfall in Ghana (1951–2000). Weather 64(5):115–120

Patie P, Winter C (2008) First exit time for multidimensional diffusions: a PDE-based approach. J Comput Appl Math 222:42–53

Spencer BF, Bergman LA (1993) On the numerical solution of the Fokker-Planck equation for nonlinear stochastic systems. Nonlinear Dyn 4:357–372

Unami K, Kawachi T, Kranjac-Berisavljevic G, Abagale FK, Maeda S, Takeuchi J (2009) Case study: hydraulic modeling of runoff processes in Ghanaian inland valleys. J Hydraul Eng ASCE 135(7):539–553

Wu SJ, Yang JC, Tung YK (2006) Identification and stochastic generation of representative rainfall temporal patters in Hong Kong territory. Stoch Environ Res Risk Assess 20:171–183